

Crystal structure of the PsbP protein of photosystem II from *Nicotiana tabacum*

Kentaro Ifuku^{1,2}, Toru Nakatsu^{2,3}, Hiroaki Kato^{2,3} & Fumihiko Sato^{1*}

¹Division of Integrated Life Science, Graduate School of Biostudies, Kyoto University, Kyoto, Japan,

²Membrane Dynamics Research Group, RIKEN Harima Institute at SPring-8, Hyogo, Japan, and ³Department of Structural Biology, Graduate School of Pharmaceutical Sciences, Kyoto University, Kyoto, Japan

PsbP is a membrane-extrinsic subunit of the water-oxidizing complex photosystem II (PS II). The evolutionary origin of PsbP has long been a mystery because it specifically exists in higher plants and green algae but not in cyanobacteria. We report here the crystal structure of PsbP from *Nicotiana tabacum* at a resolution of 1.6 Å. Its structure is mainly composed of β -sheet, and is not similar to any structures in cyanobacterial PS II. However, the electrostatic surface potential of PsbP is similar to that of cyanobacterial PsbV (cyt *c*₅₅₀), which has a function similar to PsbP. A structural homology search with the DALI algorithm indicated that the folding of PsbP is very similar to that of Mog1p, a regulatory protein for the nuclear transport of Ran GTPase. The structure of PsbP provides insight into its novel function in GTP-regulated metabolism in PS II.

Keywords: crystal structure; photosystem II; extrinsic protein; PsbP; molecular evolution

EMBO reports (2004) 5, 362–367. doi:10.1038/sj.embor.7400113

INTRODUCTION

Photosystem II (PS II) is a large multisubunit protein–pigment complex that uses light energy to split water into molecular oxygen and reducing equivalents. This water-splitting reaction takes place on the luminal side of PS II and is catalysed by a Mn cluster consisting of four redox-active Mn cations. The Mn cluster is surrounded by at least three extrinsic proteins attached to the luminal surface of PS II. These proteins comprise the oxygen-evolving complex (OEC) and have important roles in stabilizing and optimizing the water-splitting reaction (for a review, see Seidler, 1996).

In all types of oxygenic photosynthetic organisms, the membrane-extrinsic protein PsbO stabilizes the Mn cluster. PsbO is also called OEC33 because of its apparent molecular mass of 33 kDa. Plants and green algae also contain two other OEC proteins: PsbP (OEC23: 23 kDa) and PsbQ (OEC17: 17 kDa). These two proteins cooperate to optimize the levels of Ca²⁺ and Cl[−], which are essential cofactors for the water-splitting reaction (Ghanotakis & Yocum, 1985; Murata & Miyao, 1985; Ifuku & Sato, 2002). Conversely, cyanobacteria have two other OEC proteins, PsbV (15 kDa: cyt *c*₅₅₀) and PsbU (12 kDa), instead of PsbP and PsbQ (Shen *et al*, 1992). The functions of PsbV and PsbU resemble those of PsbP and PsbQ, but they differ from PsbP and PsbQ with regard to both their primary sequences and binding characteristics to the PS II complex (Shen & Inoue, 1993). These observations suggest that the replacement of PsbV and PsbU by PsbP and PsbQ occurred during the evolution of PS II, and a proposal regarding the molecular evolution of PsbQ was recently reported (Ohta *et al*, 2003). However, it is still unclear how and why PsbP evolved in higher plants.

Recently, the structural organization of cyanobacterial extrinsic proteins (PsbO, PsbV and PsbU) was revealed in the crystal structures of PS II from thermophilic cyanobacteria at resolutions of 3.8 Å (Zouni *et al*, 2001) and 3.7 Å (Kamiya & Shen, 2003). The detailed three-dimensional (3D) structure of PsbV was also reported in X-ray crystallographic studies (Frazao *et al*, 2001; Sawaya *et al*, 2001; Kerfeld *et al*, 2003). Conversely, only a relatively low-resolution structure (8 Å) is available for the PS II core from higher plants that do not contain PsbP or PsbQ (Rhee *et al*, 1998; Hankamer *et al*, 2001). The structural organization of the membrane-extrinsic proteins in higher plants has only been determined from single-particle analysis of the spinach PS II–LHCII supercomplex at a resolution of ~17 Å (Nield *et al*, 2000a,b, 2002), whereas the crystal structure of isolated PsbQ has been reported (Calderone *et al*, 2003).

In this study, we focused on PsbP, which represents the PsbP domain protein family in the Pfam database, where many paralogues in *Arabidopsis* and one orthologue in cyanobacteria have been found. However, the structural details and functions of PsbP domain proteins are still completely unknown. To elucidate the 3D structure of PsbP, the crystal structure of

¹Division of Integrated Life Science, Graduate School of Biostudies, Kyoto University, Sakyo-ku, Kyoto 606-8502, Japan

²Membrane Dynamics Research Group, RIKEN Harima Institute at SPring-8, Sayo-gun, Hyogo 679-5148, Japan

³Department of Structural Biology, Graduate School of Pharmaceutical Sciences, Kyoto University, 46-29 Yoshida Shimoauchi-cho, Sakyo-ku, Kyoto 606-8501, Japan

*Corresponding author. Tel: +81 75 753 6381; Fax: +81 75 753 6398;

E-mail: fumihiko@kais.kyoto-u.ac.jp

PsbP from *Nicotiana tabacum* was determined at a resolution of 1.6 Å.

RESULTS AND DISCUSSION

Structure of PsbP

The structure of PsbP lacking the N-terminal nine amino acids was determined by the multiwavelength anomalous diffraction (MAD) method with a Hg derivative. Fig 1 shows part of the final 1.6-Å-resolution $2F_o - F_c$ electron-density map. The electron densities of the N-terminal portion (residues 10–15) and two loop regions (residues 91–107 and 138–140) were not seen in the model because of disorder. The structure of PsbP is based on central six-stranded antiparallel β -sheet covered on both sides by α -helices (Fig 2). The segment Thr 16–Phe 53 forms an antiparallel β -sheet and one β -strand (domain I) that back the central sheet (domain II).

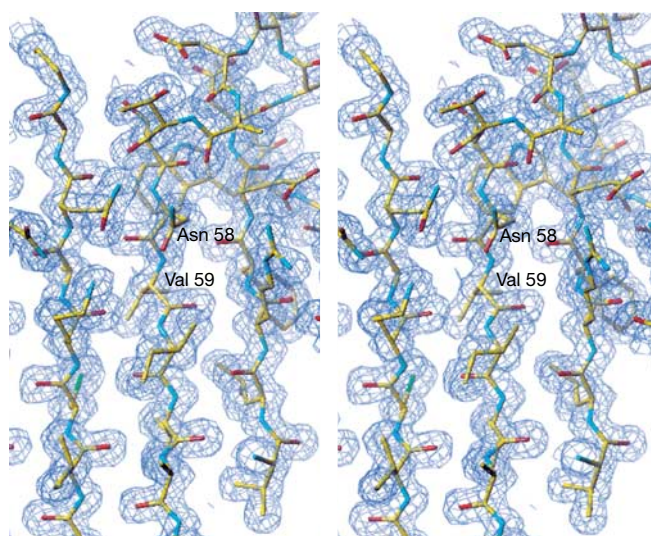


Fig 1 | Stereo view of a section of the electron-density map. The map was calculated with coefficients $2F_o - F_c$, and the refined model was superimposed. The residues of Asn 58 and Val 59 were labelled. Electron density is contoured at 1.0σ . The figure was generated with TURBO-FRODO (Roussel & Cambillau, 1996).

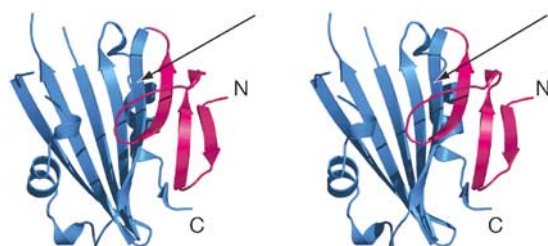


Fig 2 | Stereo view of the structure of PsbP. The schematic representation of the PsbP structural model shows a series of β -strands that are derived from residues 16–53 (domain I: pink) and the central six-stranded antiparallel β -sheet flanked on both sides by helices (domain II: blue). The N (residue 16) and C (residue 186) termini are labelled. The position of the Asn 58–Val 59 bond is indicated by an arrow. The figure was generated with PyMOL (<http://www.pymol.org>).

The existence of two distinct domains in PsbP is consistent with a previous report that showed that the Asn 58–Leu 59 bond in spinach PsbP, which corresponds to the Asn 58–Val 59 bond in tobacco PsbP, becomes susceptible to proteolysis under moderately denaturing conditions (Kuwabara & Suzuki, 1995). The exchange of domain I among PsbPs from several plant species has been shown to affect significantly the ion-retention activity of these hybrid proteins, suggesting that domain I has an important role in ion-retention activity in PS II (Ifuku & Sato, 2001). Our structural model of PsbP can hardly explain the molecular mechanism of Ca^{2+} and Cl^- retention in PS II, as it lacks the N-terminal region of PsbP, which is essential for Ca^{2+} - and Cl^- -retention activity (Ifuku & Sato, 2002). As PsbQ has been shown to compensate functionally for the N-terminal region of PsbP (Ifuku & Sato, 2002), domain I should be located near PsbQ. This N-terminal region of PsbP could adopt a native structure required for Ca^{2+} and Cl^- retention only when it is bound to the PS II core.

The C-terminal helix seems to be essential for protein folding as removal of the last ten amino acids causes a severe conformational change: the truncated PsbP is not translocated efficiently to the thylakoid lumen and degrades rapidly (Roffey & Theg, 1996). These C-terminal residues of PsbP should be important for supporting the structure of the central β -sheet in domain II.

Comparison with cyanobacterial PS II subunits

As shown in Fig 2, the structure of PsbP is mainly composed of β -sheet. Conversely, PsbV and PsbU contain mainly α -helix, and no structure similar to PsbP was found in cyanobacterial PS II, which was recently reported at a resolution of 3.7 Å (Kamiya & Shen, 2003). Among the cyanobacterial extrinsic proteins, PsbV (cyt c_{550}) resembles PsbP in terms of their roles in maintaining Ca^{2+} and Cl^- in PS II, and in their requirement for the binding of a third extrinsic protein: PsbU in cyanobacteria (Shen *et al*, 1998) and PsbQ in higher plants (Miyao & Murata, 1989). Furthermore, both proteins are located near the luminal side of the membrane-intrinsic proteins D1, CP43 and cyt b_{559} (Nield *et al*, 2000a,b, 2002; Kamiya & Shen, 2003).

We then compared the electrostatic surface potentials of the 3D structures of PsbP and PsbV to discern any similarity between them. PsbV has an asymmetric charge distribution with pronounced positively and negatively charged surfaces (Sawaya *et al*, 2001; Fig 3B). PsbP also has a basic surface with conserved positively charged amino acids (Arg48, Lys143 and Lys160), whereas other surfaces are rather acidic (Fig 3A). In cyanobacterial PS II, PsbV directly associates with the membrane-intrinsic proteins, but does not directly interact with PsbO (Kamiya & Shen, 2003); the positively charged surface interacts with portions of the intrinsic proteins that protrude from the membrane surface, and the negatively charged surface interacts with PsbU. The exact binding site on the PS II core could be different between the two proteins (Enami *et al*, 2000). However, both proteins are known to bind to PS II with electrostatic interaction, and the luminal surface of thylakoid membrane from higher plants has been shown to be acidic (Åkerlund *et al*, 1979). Thus, it is reasonable to assume that the basic surface of PsbP would interact with the PS II core in a manner similar to PsbV in cyanobacterial PS II. A direct interaction between PsbP and PS II membrane-intrinsic subunits has been suggested by *in vitro* experiments (Yamamoto, 1988), and PsbP in *Chlamydomonas* can bind to PS II directly, although

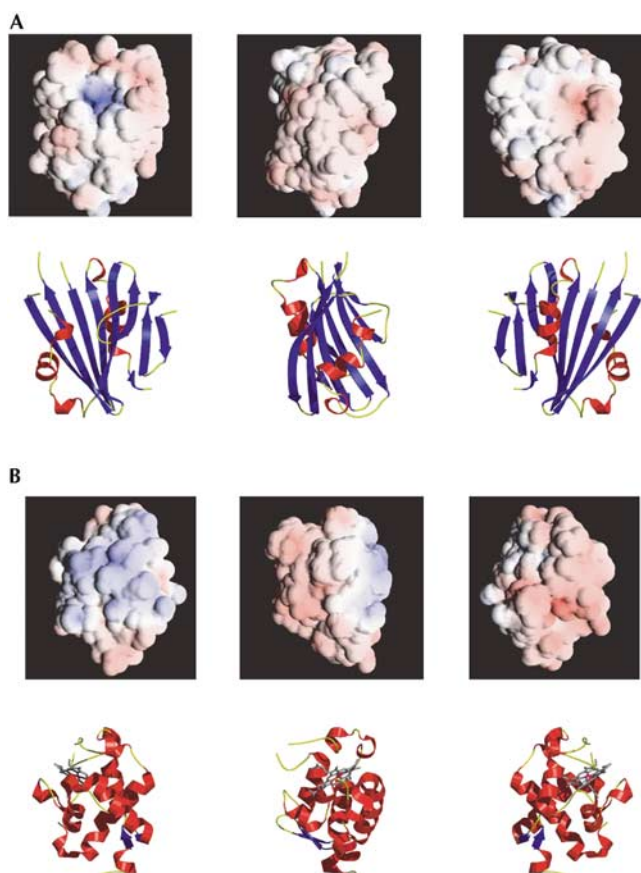


Fig 3 | Comparison of the electrostatic surface potentials of (A) PsbP from *N. tabacum* (this study) and (B) PsbV from *Thermosynechococcus elongatus* (Kerfeld *et al*, 2003). The molecules are rotated anticlockwise by 90° and 180° around a vertical axis (left to right). The figure was produced using GRASP (Nicholls *et al*, 1991).

PsbO is necessary to activate PS II activity (de Vitry *et al*, 1989; Suzuki *et al*, 2003). Recent reports have shown that PS II isolated from transgenic tobacco with low *cyt b₅₅₉* content did not have any bound PsbP, whereas a significant amount of PsbP was present in the thylakoid lumen (Bondarava *et al*, 2003). Other regions of PsbP (particularly, the negatively charged regions) might interact with PsbQ, which has many positively charged residues on its surface (Calderone *et al*, 2003), and with PsbO, which is indispensable for the stable and functional binding of PsbP to isolated PS II *in vitro* (Miyao & Murata, 1989).

Structural similarity to a Ran-GTPase-binding protein

The absence of a PsbP-like protein in cyanobacterial PS II suggests that the extrinsic proteins of higher plants and green algae began to diverge from those in cyanobacteria primarily during the evolution of PS II. A structural homology search with the DALI algorithm showed that PsbP is folded very similarly to Mog1p (1EQ6; Z score 11.3), which is a regulatory protein for the nuclear transport of Ran GTPase in yeast (Oki & Nishimoto, 1998; Stewart & Baker, 2000) (Fig 4A). PsbP is not likely to be a 'Ran-binding protein', as the amino-acid sequences have low identity and the insertions and deletions in loop regions are different between the

two proteins (Fig 4B). Our biochemical analysis also failed to detect an interaction of PsbP with human Ran GTPase (data not shown). However, the structural similarity provides a framework for investigating the unknown functions of PsbP and other PsbP domain proteins in higher plants and cyanobacteria. Such investigations may also provide insight into the evolutionary origin of PsbP.

Speculation

The strong structural similarity between PsbP and Mog1p allows us to speculate why higher plants use PsbP instead of PsbV. In higher plants, GTP stimulates degradation of the photodamaged PS II reaction centre D1 protein (Spetea *et al*, 1999), and PsbO has been identified as a GTP-binding protein (Spetea *et al*, 2001). However, D1 degradation has been reported to be dependent on GTP only in higher plants, and the process of D1 degradation has been reported to differ between higher plants and cyanobacteria (Silva *et al*, 2003). Mog1p stimulates nucleotide release from Ran GTPase and modulates its nucleotide state (Baker *et al* 2001). Thus, we can speculate that when higher plants acquired GTP-dependent regulation in D1 metabolism, they may have also acquired PsbP to modulate the nucleotide state of PsbO instead of PsbV, which does not interact with PsbO directly. The precise biological roles of GTP bound to PsbO should be investigated.

METHODS

Purification, crystallization and preparation of the Hg derivative.

PsbP from *N. tabacum* was expressed in *Escherichia coli*, purified and crystallized as described previously (Ifuku *et al*, 2003). The nine amino-terminal residues of PsbP were genetically removed because these residues have been shown to be easily degraded during crystallization and are functionally dispensable (Miyao *et al*, 1988; Ifuku *et al*, 2003). For phase determination, an ethylmercurithiosalicylate (EMTS) derivative was prepared by soaking the native crystal in mother liquor containing 0.1 mM EMTS, 0.1 M lithium sulphate, 30% (w/v) PEG4000 and 50 mM MES buffer (pH 6.0) for 3 days.

Data collection. The native crystal was flash-frozen in liquid nitrogen after being soaked in a cryoprotectant solution containing 35% (w/v) PEG4000, 5% (w/v) sucrose and 5% (w/v) glucose in 50 mM MES buffer (pH 6.0). X-ray data were collected on beamline BL44B2 at SPring-8 using a marCCD165 detector at 90 K. The crystals belong to space group $P2_12_12$ with $a=74.5$, $b=90.4$ and $c=52.6$ Å, and diffract to a resolution of 1.6 Å. In the case of the Hg derivative, the Hg-soaked crystal was back-soaked and flash-frozen in liquid nitrogen using cryoprotectant solution. An X-ray fluorescence spectrum was measured directly from the crystal on the BL45XU beamline at SPring-8 using a Si diode X-ray fluorescence detector. The remote wavelength used was 1.035 Å, and the peak and inflection were 1.00907 and 1.0072 Å, respectively. MAD data sets were collected from 0° to 180° with 1° oscillation on the BL45XU beamline at SPring-8 using a Jupiter210 CCD detector at 90 K. Three data sets were collected in the order peak, edge and remote per ten frames, and the exposure times were 10, 5 and 5 s, respectively. MAD data were collected to a resolution of at least 1.9 Å. The space group of the Hg-derivative crystals changed to space group $P2_1$, with $a=73.9$, $b=90.6$, $c=52.4$ Å and $\beta=90^\circ$. The native and derivative data

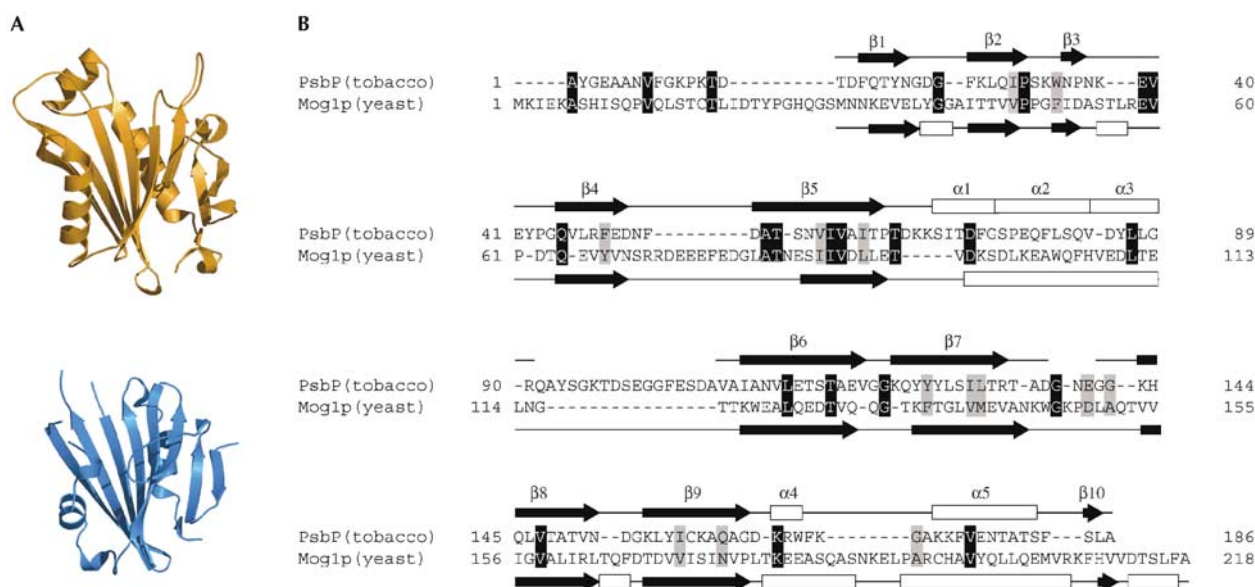


Fig 4 | Structural similarity between PsbP and Mog1p. (A) Structures of Mog1p from *Saccharomyces cerevisiae* (top; Stewart & Baker, 2000) and PsbP from *N. tabacum* (bottom; this study). (B) Structure-based sequence alignment of tobacco PsbP and yeast Mog1p. GenBank/EMBL/DDDBJ database accession numbers are CAA44293 and P47123, respectively.

Table 1 | Statistics of X-ray data collection

	Native	Hg derivative		
		Remote	Peak	Inflection
Space group	$P2_12_12_1$	$P2_1$	-	-
Cell dimensions (Å)	74.5, 90.4, 52.6	73.9, 90.6, 52.4	-	-
β (deg)	-	90	-	-
Wavelength (Å)	1.0	1.035	1.00907	1.00720
Resolution (Å)	52.6–1.6	50–1.9	50–1.9	50–1.9
Unique reflections ^a	47,044	54,456	54,473	54,456
Redundancy	7.3	3.8	3.8	3.8
Completeness (%)	98.7 (97.3)	99.1 (90.3)	99.2 (92.0)	99.2 (91.8)
$I/\sigma(I)$	7.8 (2.4)	10.6 (4.3)	10.6 (4.2)	10.6 (4.3)
R_{merge} (%)	7.3 (30.7)	4.2 (12.0)	4.1 (12.6)	4.2 (13.6)

Data for the outer shell are in parentheses.

^aIncrease in the number of reflections in Hg derivative was due to the difference of space groups between native crystal and Hg derivative.

sets were integrated and scaled with Crystal Clear (Rigaku/MS; Pflugrath, 1999). Data collection statistics are given in Tables 1,2. **MAD phasing, automatic model building and refinement.** The Hg sites were determined, refined and used for phase calculation in the program SOLVE (Terwilliger & Berendzen, 1999). Phases were improved with RESOLVE (Terwilliger, 2000), resulting in an overall figure of merit of 0.65. The initial model was constructed automatically by ARP/wARP (Perrakis *et al*, 1999) with Hg-derivative data. Owing to the difference in the space group between native and Hg-derivative crystals, molecular replacement was carried out with AMoRe (Navaza, 1994) using the initial

model obtained by ARP/wARP. The warpNtrace mode of ARP/wARP then automatically built a model that had 149 of 177 amino-acid residues of PsbP in the native electron density at a resolution of 1.6 Å. Water molecules were added with the solvent mode of ARP/wARP. The remaining parts of the structure were built manually using the program TURBO-FRODO (Roussel & Cambillau, 1996), and the resulting model was refined by Refmac (Murshudov *et al*, 1997). Refinement statistics are given in Table 1.

Protein Data Bank accession numbers. The atomic coordinates and structure factors of the tobacco PsbP protein have been

Table 2 | Statistics of X-ray refinement

Resolution range (Å)	20–1.6
R_{work} (%)	18.6
R_{free} (%)	20.7
Protein atoms	2,357
Hetero-atoms ^a	34
Solvent atoms	433
Average B -factor (Å ²)	13.5
$\phi\psi$ most favoured	94.5
$\phi\psi$ additionally allowed	5.5
R.m.s. deviation from ideal values	
Bond length (Å)	0.006
Bond angle (deg)	0.95

R_{free} is the R_{factor} with 5% of the reflections excluded from refinement.
^aThese atoms are from sulphate ion and glucose that were included in a cryoprotectant solution.

deposited in the Protein Data Bank under accession number 1V2B.

ACKNOWLEDGEMENTS

We thank Dr M. Yamamoto, Dr T. Kumasaka and Dr S. Adachi for their assistance in X-ray data collection on the RIKEN beamlines at SPring-8. This work was supported in part by a Research for the Future Program Grant (JSPS-RFTF 00L01606) from the Japan Society for the Promotion of Science to F.S., and by a Grant-in-Aid for Scientific Research from the Ministry of Education, Sports, and Culture of Japan to K.I. (15770026).

REFERENCES

- Åkerlund H-E, Andersson B, Persson A, Albertson P-A (1979) Isoelectric points of spinach thylakoid membrane surfaces as determined by cross partition. *Biochim Biophys Acta* **552**: 238–246
- Baker RP, Harreman MT, Eccleston JF, Corbett AH, Stewart M (2001) Interaction between Ran and Mog1 is required for efficient nuclear protein import. *J Biol Chem* **276**: 41255–41262
- Bondarava N et al (2003) Evidence that cytochrome b_{559} mediates the oxidation of reduced plastoquinone in the dark. *J Biol Chem* **278**: 13554–13560
- Calderone V et al (2003) Crystal structure of the PsbQ protein of photosystem II from higher plants. *EMBO Rep* **4**: 900–905
- de Vitry C, Olive J, Drapier D, Recouvreur M, Wollman FA (1989) Post-translational events leading to the assembly of photosystem II protein complex: a study using photosynthesis mutants from *Chlamydomonas reinhardtii*. *J Cell Biol* **109**: 991–1006
- Enami I, Yoshihara S, Tohri A, Okumura A, Ohta H, Shen J-R (2000) Cross-reconstitution of various extrinsic proteins and photosystem II complexes from cyanobacteria, red algae and higher plants. *Plant Cell Physiol* **41**: 1354–1364
- Frazao C et al (2001) Crystal structure of low-potential cytochrome c_{549} from *Synechocystis* sp. PCC 6803 at 1.21 Å resolution. *J Biol Inorg Chem* **6**: 324–332
- Ghanotakis DF, Yocum CF (1985) Polypeptides of photosystem II and their role in oxygen evolution. *Photosynth Res* **7**: 97–114
- Hankamer B, Morris E, Nield J, Gerle C, Barber J (2001) Three-dimensional structure of the photosystem II core dimer of higher plants determined by electron microscopy. *J Struct Biol* **135**: 262–269
- Ifuku K, Sato F (2001) Importance of the N-terminal sequence of the extrinsic 23 kDa polypeptide in photosystem II in ion-retention in oxygen-evolution. *Biochim Biophys Acta* **1546**: 196–204
- Ifuku K, Sato F (2002) A truncated mutant of the extrinsic 23-kDa protein that absolutely requires the extrinsic 17-kDa protein for Ca^{2+} retention in photosystem II. *Plant Cell Physiol* **43**: 1244–1249
- Ifuku K, Nakatsu T, Kato H, Sato F (2003) Crystallization and preliminary crystallographic studies on the extrinsic 23 kDa protein in the oxygen-evolving complex of photosystem II. *Acta Crystallogr D* **59**: 1462–1463
- Kamiya N, Shen J-R (2003) Crystal structure of oxygen-evolving photosystem II from *Thermosynechococcus vulcanus* at 3.7-Å resolution. *Proc Natl Acad Sci USA* **100**: 98–103
- Kerfeld et al (2003) Structural and EPR characterization of the soluble form of cytochrome c -550 of the *psbV2* gene product from cyanobacterium *Thermosynechococcus elongatus*. *Plant Cell Physiol* **44**: 697–706
- Kuwabara T, Suzuki K (1995) Reversible changes in conformation of the 23-kDa protein of photosystem II and their relationship to the susceptibility of the protein to a proteinase from photosystem II membranes. *Plant Cell Physiol* **36**: 495–504
- Miyao M, Murata N (1989) The mode of binding of three extrinsic proteins of 33 kDa, 23 kDa, and 18 kDa in Photosystem II complex of spinach. *Biochim Biophys Acta* **977**: 315–321
- Miyao M, Fujimura Y, Murata N (1988) Partial degradation of the 23-kDa protein of the Photosystem II complex of spinach. *Biochim Biophys Acta* **936**: 465–474
- Murata N, Miyao M (1985) Extrinsic membrane proteins in the photosynthetic oxygen-evolving complex. *Trends Biochem Sci* **10**: 122–124
- Murshudov GN, Vagin AA, Dodson EJ (1997) Refinement of macromolecular structures by the maximum-likelihood method. *Acta Crystallogr D* **53**: 240–255
- Navaza J (1994) AMoRe: an automated package for molecular replacement. *Acta Crystallogr A* **50**: 157–163
- Nicholls A, Sharp KA, Honig B (1991) Protein folding and association: insights from the interfacial and thermodynamic properties of hydrocarbons. *Proteins* **11**: 281–296
- Nield J, Orlova EV, Morris EP, Gowen B, van Heel M, Baber J (2000a) 3D map of the plant photosystem II supercomplex obtained by cryoelectron microscopy and single particle analysis. *Nat Struct Biol* **7**: 44–47
- Nield J, Kruse O, Ruprecht J, da Fonseca P, Buchel C, Barber J (2000b) Three-dimensional structure of *Chlamydomonas reinhardtii* and *Synechococcus elongatus* photosystem II complexes allows for comparison of their oxygen-evolving complex organization. *J Biol Chem* **275**: 27940–27946
- Nield J, Balsera M, Las Rivas JD, Barber J (2002) 3D cryo-EM study of the extrinsic domains of the oxygen evolving complex of spinach: assignment of the PsbO protein. *J Biol Chem* **277**: 15006–15012
- Ohta H et al (2003) Extrinsic proteins of photosystem II. *Eur J Biochem* **270**: 4156–4163
- Oki M, Nishimoto T (1998) A protein required for nuclear-protein import, Mog1p, directly interacts with GTP-Gsp1p, the *Saccharomyces cerevisiae* ran homologue. *Proc Natl Acad Sci USA* **95**: 15388–15393
- Perrakis A, Morris R, Lamzin VS (1999) Automated protein model building combined with interactive structure refinement. *Nat Struct Biol* **6**: 458–463
- Pflugrath JW (1999) The finer things in X-ray diffraction data collection. *Acta Crystallogr D* **55**: 1718–1725
- Rhee K-H, Morris EP, Baber J, Kühlbrandt W (1998) Three-dimensional structure of the plant photosystem II reaction centre at 8 Å resolution. *Nature* **396**: 283–286
- Roffey RA, Theg SM (1996) Analysis of the import of carboxyl-terminal truncations of the 23-kilodalton subunit of the oxygen-evolving complex suggests that its structure is an important determinant for thylakoid transport. *Plant Physiol* **111**: 1329–1338
- Roussel A, Cambillau C (1996) *TURBO-FRODO Manual*. Marseille, France: AFMB-CNRS
- Sawaya MR, Krogmann DW, Serag A, Ho KK, Yeates TO, Kerfeld CA (2001) Structures of cytochrome c -549 and cytochrome c_6 from the cyanobacterium *Arthrospira maxima*. *Biochemistry* **7**: 9215–9225
- Seidler A (1996) The extrinsic polypeptides of photosystem II. *Biochim Biophys Acta* **1277**: 35–60
- Shen J-R, Inoue Y (1993) Binding and functional properties of two new extrinsic components, cytochrome c_{550} and 12 kDa protein, in cyanobacterial photosystem II. *Biochemistry* **32**: 1925–1932
- Shen J-R, Ikeuchi M, Inoue Y (1992) Stoichiometric association of extrinsic cytochrome c_{550} and 12 kDa protein with a highly purified oxygen-

- evolving photosystem II core complex from *Synechococcus vulcanus*. *FEBS Lett* **301**: 145–149
- Shen J-R, Qian M, Inoue Y, Burnap RL (1998) Functional characterization of *Synechocystis* sp. PCC 6803 delta psbU and delta psbV mutants reveals important roles of cytochrome *c*-550 in cyanobacterial oxygen evolution. *Biochemistry* **37**: 1551–1558
- Silva P et al (2003) FtsH is involved in the early stages of repair of photosystem II in *Synechocystis* sp. PCC 6803. *Plant Cell* **15**: 2152–2164
- Spetea C, Hundal T, Lohmann F, Andersson B (1999) GTP bound to chloroplast thylakoid membranes is required for light-induced, multienzyme degradation of the photosystem II D1 protein. *Proc Natl Acad Sci USA* **96**: 6547–6552
- Spetea C, Hundal T, Andersson B (2001) The 33 kDa subunit of photosystem II is a GTP-binding protein—presence of nucleotides in the thylakoid lumen. In *PS2001 Proceedings, 12th International Congress on Photosynthesis*, (Online and CD-ISBN 0643-067116), S8-005
- Stewart M, Baker RP (2000) 1.9 Å resolution crystal structure of the *Saccharomyces cerevisiae* Ran-binding protein Mog1p. *J Mol Biol* **299**: 213–223
- Suzuki T, Minagawa J, Tomo T, Sonoike K, Ohta H, Enami I (2003) Binding and functional properties of the extrinsic proteins in oxygen-evolving photosystem II particle from a green alga, *Chlamydomonas reinhardtii* having his-tagged CP47. *Plant Cell Physiol* **44**: 76–84
- Terwilliger TC (2000) Maximum likelihood density modification. *Acta Crystallogr D* **56**: 965–972
- Terwilliger TC, Berendzen J (1999) Automated MAD and MIR structure solution. *Acta Crystallogr D* **55**: 849–861
- Yamamoto Y (1988) Organization of the oxygen-evolution enzyme complex studied by butanol/water phase partitioning of spinach photosystem II particles. *J Biol Chem* **263**: 497–500
- Zouni A et al (2001) Crystal structure of photosystem II from *Synechococcus elongatus* at 3.8 Å resolution. *Nature* **409**: 739–743